Analysis of low energy π^+ scattering to second O^+ states

R. Alvarez del Castillo and N. B. de Takacsy
Department of Physics, McGill University, 3600 University Street, Montreal, Quebec, Canada H3A 2T8
(Received 10 July 1990)

An optical potential with a strong Ericson-Ericson-Lorentz-Lorenz parameter is used to calculate low-energy pion inelastic scattering to selected collective states and excited 0^+ states in ^{12}C and ^{28}Si. The nuclear structure input is carefully evaluated, and there are no free parameters in the calculation. The scattering to the 0_2^+ states proceeds dominantly through the one-step mechanism, but the two-step mechanism is significant and can be used to extract some information about the form factors connecting excited states.

I. INTRODUCTION

If one makes a naive use of the experimental π-nucleon-scattering cross sections, one would expect that a low-energy (~ 50 MeV) pion would be a weakly interacting nuclear probe. On the other hand, if one translates the same data into an optical potential of the Kisslinger type, one can end up with very strong multiple scattering in the π-nucleus interaction. The corresponding high-momentum components in the wave function must then be suppressed by a variety of mechanisms, which are collectively referred to as the Ericson-Ericson-Lorentz-Lorenz (EELL) effect and which can be approximately incorporated into the π-nucleus optical potential through a single parameter.[1] Unfortunately, it has proved difficult to extract this parameter unambiguously from the data. It has been argued[2] that inelastic scattering of low-energy pions to second 0^+ states provides one way of attacking this question: the point is that the form factor must have a vanishing volume integral for orthogonality reasons, and this results in a depression of the differential cross section at forward angles for weakly interacting probes. On the other hand, such a decrease can also result from the interference between the one-step $0_1^+ \to 0_2^+$ and the two-step $0_1^+ \to 2_1^+ \to 0_2^+$ amplitudes.[3,4] The arguments are model dependent: Potentials that generate strong multiple scattering in the elastic channel will also generate strong two-step amplitudes, and conversely for potentials with large EELL parameters.

For a long time, inelastic-scattering data to a 0_2^+ state was available only for ^{12}C.[5,6] Very recently, much better energy resolution has become available at LAMPF, and an experiment was performed on ^{28}Si at 50 MeV.[7] This is very useful data because the nuclear structure is much better understood here than in ^{12}C. Moreover, new data on ^{12}C has also been taken.[8,9]

The purpose of this paper is to do a unified analysis of all the low-energy data for pion scattering to second 0^+ states, and, among other things, to draw a clear conclusion about the relative importance of one- and two-step amplitudes. For completeness and consistency, we also calculate elastic and inelastic scattering to the first 2^+ and 4^+ states, and show that they are correctly predicted without any adjustable parameter.

II. π-NUCLEUS INTERACTION

Elastic scattering is calculated in the usual way by solving the Klein-Gordon equation with an optical potential of standard form, but restricted to $N=Z$ nuclei, and proton and neutron densities having the same shape:

$$2\omega V = u_0 + U_0 + \nabla\left[\frac{u_1}{(1+\lambda u_1/3)} + U_1\right]\nabla + \frac{\omega}{2m_n}[\nabla^2(u_1+\tfrac{1}{2}U_1)] , \quad (1)$$

$$u_0 = -4\pi_1 A b_0 \rho , \quad (2)$$

$$U_0 = -4\pi p_2 A^2 B_0 \rho^2 , \quad (3)$$

$$u_1 = 4\pi A c_0 \rho / p_1 , \quad (4)$$

$$U_1 = 4\pi A^2 C_0 \rho^2 / p_2 , \quad (5)$$

$$p_1 = 1+\omega/m_n , \quad (6)$$

$$p_2 = 1+\omega/2m_n . \quad (7)$$

We use the low-energy parametrization of Meirav *et al.* [10] which is the best available at the moment, and which is summarized in Table I. This is a potential with a "strong" EELL parameter.

Inelastic scattering to $J_f \neq 0$ states is calculated assuming a one-step distorted-wave Born approximation (DWBA) mechanism using a much modified version of the code NDWPI.[11] Inelastic scattering to the 0_2^+ states is calculated as a coherent sum of one-step $(0_1^+ \to 0_2^+)$ and two-step $(0_1^+ \to 2_1^+ \to 0_2^+)$ amplitudes using a homemade code BORNOJO. For inelastic vertices, the transition operator is taken to be that piece of

$$2\omega\delta V = 2\omega(V\{\rho+\delta\rho\} - V\{\rho\}) , \quad (8)$$

which is linear in $\delta\rho$.

The diagonal and off-diagonal transition densities are the point nucleon densities and are obtained, as far as possible, by unfolding the finite proton size from electromagnetic data: longitudinal electron scattering form factors, and $B(E2)$ and $M(0)$ values from γ decay or Coulomb scattering.

TABLE I. The π-nucleus optical potential parameters.

T_π	$b_0(m_\pi^{-1})$	$c_0(m_\pi^{-3})$	$B_0(m_\pi^{-4})$	$C_0(m_\pi^{-6})$	λ
50	−0.021;0.0	0.231;0.051	−0.075;0.036	0.036;0.053	1.8
65	−0.026;0.0	0.237;0.087	−0.025;0.025	0.025;0.038	1.8

For computational convenience, we use standard analytic forms (specified below) fitted to the experimental densities and form factors. There is no loss of accuracy resulting from the choice of simple forms for this purpose.

III. NUCLEAR STRUCTURE OF ^{28}Si

A three-parameter Fermi ($3pf$) shape is used for the ground-state density

$$\rho(\mathbf{r})=\frac{\rho_0[1+\omega(r/c)^2]}{1+\exp[(r-c)/z]} \tag{9}$$

with the parameters fitted to the known charge density[12] after folding in the proton charge density. As expected, the point nucleon and the charge density have almost the same radius, but different surface thickness.

For $0_1^+\rightarrow 2_1^+$ and $0_1^+\rightarrow 4_1^+$ transitions, we use collective model form factors:

$$\delta\rho(\mathbf{r})=\beta_l(2l+1)^{-1/2}Y^*_{l,m}(\theta,\phi)f_l(r)\ , \tag{10}$$

$$f_l(r)=-r\frac{d}{dr}\rho(r) \tag{11}$$

with a $3pf$ form for ρ. The parameters c, z, w, and β_l are obtained by fitting (after folding) the longitudinal electron scattering form factors[13–15] and the experimental

$$B(E2;0_1^+\rightarrow 2_1^+)=326\,e^2\,\mathrm{fm}^4$$

(Ref. 16), and

$$B(E4;0_1^+\rightarrow 4_1^+)=1.78\times 10^4\,e^2\,\mathrm{fm}^8$$

(Ref. 15). We found that the conventional procedure of using the ground-state values of the parameters c, z, and w and adjusting β_2 to the experimental $B(E2)$ gives a form factor that peaks at too low a momentum transfer, and is too weak in the region of the peak when compared to the electron-scattering data. Since pion inelastic scattering around 50 MeV involves momentum transfers characteristic of this peak region, it is important to get this right. In other words, if one uses the ground-state values for c, w, and z, one should expect that the β_2 needed to fit the pion inelastic cross section will be systematically and significantly larger than the β_2 deduced from γ decay. This has been the case with most fits up to now; see, for example, Refs. 7 and 4.

For the $0_1^+\rightarrow 0_2^+$ form factors, we use the form suggested by the collective model[17] of β-vibrational states.

$$\delta\rho_0(\mathbf{r})=(4\pi)^{-1/2}\beta_0 f_0(r)\ , \tag{12}$$

$$f_0(r)=r\frac{d}{dr}\rho+\tfrac{1}{4}r^2\frac{d^2}{dr^2}\rho\ . \tag{13}$$

We again take ρ to have a $3pf$ form, and fit the four parameters to the electron-scattering data.[13]

We now complete the nuclear structure input by noting that all the states relevant to this work are good $1s$, $0d$ shell states,[18,19] and deformed Hartree-Fock calculations long ago showed that the 0_2^+ state could be interpreted as a β-vibrational state.[20] Consequently, the diagonal densities of the 2_1^+ and the 0_2^+ states are taken equal to the ground-state density, and the $0_2^+\rightarrow 2_1^+$ form factor is given the same shape as the $0_1^+\rightarrow 2_1^+$ form factor, with the corresponding β_2' derived from the known lifetime of the 0_2^+ state: $t_{1/2}=21$ fs.[21] Actually, this is something of an upper limit on β_2' since, if all the data is included instead of just the two more accurate Doppler-shift measurements, then $t_{1/2}$ increases to 31 fs.[22] Finally, the relative phases are defined by the relation $\beta_0=(2/\sqrt{\pi})\beta_2\beta_2'$ which holds in the small vibration limit of the collective model. All the nuclear structure parameters are listed in Table II.

TABLE II. Form-factor parameters.

Nucleus	Transition	Form factor	c	z	w	β_{em}
^{12}C	$0_1^+\rightarrow 0_1^+$	$3pf$	2.002	0.383	0.540	
^{12}C	$0_1^+\rightarrow 2_1^+$	$-r\frac{d}{dr}3pf$	1.921	0.428	−0.160	0.65
^{12}C	$0_1^+\rightarrow 0_2^+$	coll.,$3pf$	1.282	0.520	−0.075	0.34
^{12}C	$0_2^+\rightarrow 2_1^+$	$-r\frac{d}{dr}3pf$	1.921	0.428	−0.160	0.38
^{12}C	$0_2^+\rightarrow 2_1^+$	Kamimura				1.52
^{12}C	$0_2^+\rightarrow 0_2^+$	$3pf$	1.688	1.212	−0.039	
^{28}Si	$0_1^+\rightarrow 0_1^+$	$3pf$	3.361	0.485	−0.245	
^{28}Si	$0_1^+\rightarrow 2_1^+$	$-r\frac{d}{dr}3pf$	2.775	0.408	0.653	0.39
^{28}Si	$0_1^+\rightarrow 4_1^+$	$-r\frac{d}{dr}3pf$	3.170	0.458	−0.209	0.21
^{28}Si	$0_1^+\rightarrow 0_2^+$	coll.,$3pf$	2.476	0.361	1000	0.091
^{28}Si	$0_2^+\rightarrow 2_1^+$	$-r\frac{d}{dr}3pf$	2.775	0.408	0.653	0.19

IV. ^{28}Si $(\pi^+,\pi^{+\prime})$ REACTION

Figures 1–4 show that all the ^{28}Si$(\pi^+,)$ data are well reproduced using only one-step DWBA with an optical potential based on a strong EELL parameter and the nuclear structure input taken from electromagnetic data. There are no free parameters in the calculation.

As shown in Fig. 4, the two-step $(0_1^+ \rightarrow 2_1^+ \rightarrow 0_2^+)$ amplitude is smaller than the one-step amplitude by a factor of 2 even at small angles, but the interference between the two amplitudes has a significant effect which goes in the direction of improving the agreement with experiment, if the relative sign of the two amplitudes is taken from theory. This result is in contrast to the conclusions of Ref. 7 who find that the two-step amplitude dominates at forward angles. The difference between the two results is primarily due to our use of a better optical potential, better form factors, and a more reasonable (i.e., experimental) value for the β_2' connecting the 2_1^+ and 0_2^+ states. If we use the potentials and parameters of Ref. 7, we get results very close to theirs, from which we conclude that there is little difference between coupled-channels and one-plus-two–step DWBA calculations in this case.

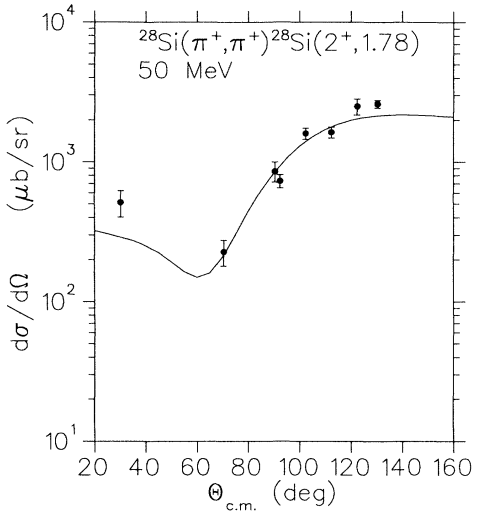

FIG. 2. Inelastic (one-step only) differential cross sections for ^{28}Si$(\pi^+,\pi^{+\prime})^{28}Si(2^+,1.78$ MeV) at 50 MeV. The data are from Refs. 7 and 29.

V. NUCLEAR STRUCTURE OF ^{12}C

For the ground-state density, and the $0_1^+ \rightarrow 2_1^+$ and $0_1^+ \rightarrow 0_2^+$ form factors, we can use the same functional forms as in ^{28}Si, with all the parameters determined by the (e,e') data.[12,23] It would be tempting to use the same approach as in ^{28}Si for the rest of the form factors as well, but the available nuclear structure information does not allow this. All theoretical models agree that the 0_1^+ and 2_1^+ states are members of the same oblate ground-state band, and that their dominant components can be attributed to the $0p$ shell. It follows that the diagonal density for the 2_1^+ state can be taken the same as the ground-state density. On the other hand, shell-model calculations[24,25] do not provide any candidate for the 0_2^+ state which must therefore be attributed to configurations beyond the $0p$ shell.

One model that provides a state space large enough to include all the states relevant for our purposes is the cluster model. There is a price paid in that the N-N forces that can be used are more crude than those of the shell model, and important spin-orbit effects cannot be accomidated. Nevertheless, form factors have been calculated in this formalism by Kamimura.[26] The description of the 0_1^+ and 2_1^+ states is much the same as in the shell model, except that they are more deformed. The 0_2^+ state is

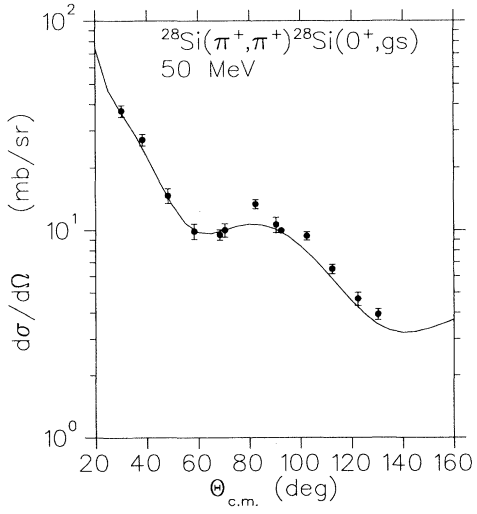

FIG. 1. Elastic (optical model) differential cross sections for ^{28}Si(π^+,π^+) at 50 MeV. The data are from Refs. 7 and 29.

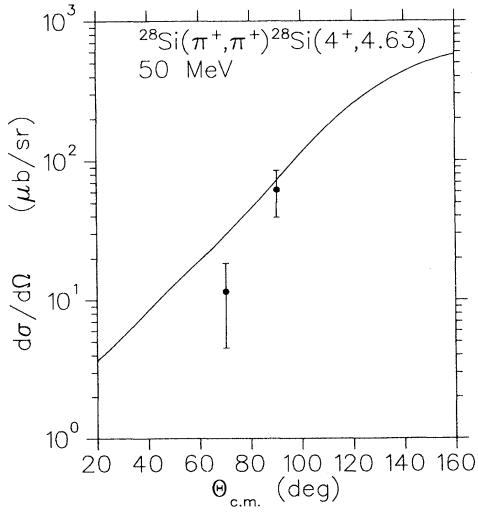

FIG. 3. Inelastic (one-step only) differential cross sections for ^{28}Si$(\pi^+,\pi^{+\prime})^{28}Si(4^+,4.63$ MeV) at 50 MeV. The data are from Refs. 7 and 29.

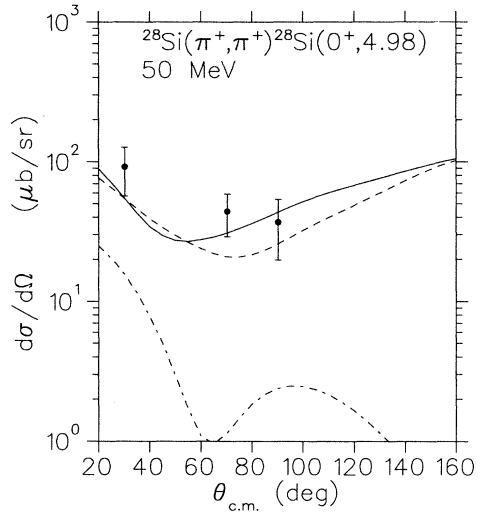

FIG. 4. Inelastic differential cross sections for ^{28}Si($\pi^+,\pi^{+\prime}$)^{28}Si(0$^+$,4.98 MeV) at 50 MeV. The dashed line is a purely one-step calculation, the dot-dashed line is a purely two-step ($0_1^+ \rightarrow 2_1^+ \rightarrow 0_2^+$) calculation, and the solid line is the coherent sum of the two mechanisms. The data are from Refs. 7 and 29.

highly deformed and mostly prolate; consequently, its density is much lower and more spread out than the ground-state density. A standard three-parameter Fermi shape provides a reasonable and convenient representation of the shape given in Ref. 26, with the parameters listed in Table II. The Kamimura form factor for the

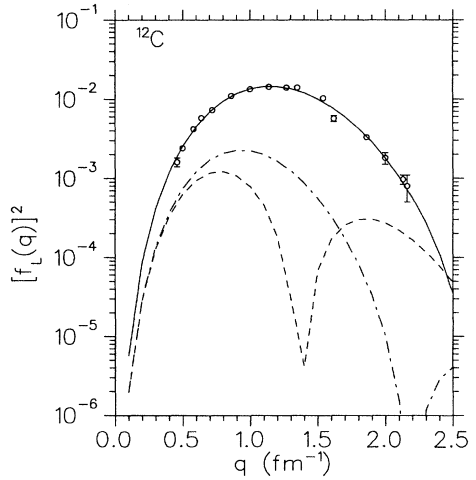

FIG. 5. The charge form factors squared in ^{12}C obtained by folding the finite proton size (Ref. 30) into the matter distributions discussed in the text. The solid line is for the $0_1^+ \rightarrow 2_1^+$ transition with the parameters given in Table II, and the data is from Ref. 23. The dashed line is Kamimura's form factor (Ref. 26) for the $0_2^+ \rightarrow 2_1^+$ transition, multiplied by 1.52 to make the magnitude consistent with the measured $B(E2)$ (Ref. 28). The dot-dashed line show the $0_2^+ \rightarrow 2_1^+$ form factor with $\beta_2'=0.8$, and $\beta_2''=0.18$, which is preferred by the pion inelastic-scattering data.

$0_2^+ \rightarrow 2_1^+$ transition has a shape that is totally different from that of the $0_1^+ \rightarrow 2_1^+$ transition; see Fig. 5. Its phase is the same at low q^2, but it has a node and changes sign at high q^2. It underestimates the $B(E2;0_2^+ \rightarrow 2_1^+)$ by more than a factor of 2 and this is sensitive to the choice of nucleon-nucleon potential—other calculations give even smaller numbers.[27] For the present purposes, we take the $0_2^+ \rightarrow 2_1^+$ form factor to be a linear combination of the Kamimura form factor (Kam) and the β-vibrational form factor:

$$f_2(0_2^+ \rightarrow 2_1^+;r)=\beta_2' f_2(\text{Kam};r)+\beta_2'' f_2(0_1^+ \rightarrow 2_1^+;r) \ . \tag{14}$$

The coefficients will be varied subject to the constraint that

$$B(E2;0_2^+ \rightarrow 2_1^+)=13\pm4\, e^2\,\text{fm}^4$$

(Ref. 28).

VI. ^{12}C ($\pi^+,\pi^{+\prime}$) REACTION

As shown in Figs. 6 and 7, the DWBA cross section for the 2_1^+ state is in good agreement with the data;[31,8,9] in particular, there is no need to change the electromagnetic value of β_2. The one-step DWBA cross sections for the 0_2^+ state are shown in Figs. 8–10. They agree with the data at both 50 and 67.5 MeV but only for $\theta > 70°$. The shape of the angular distributions shows the suppression at forward angles characteristic of weakly interacting particles, and the low nuclear density of the final state is significant in this regard. Nevertheless, the data require more suppression than the one-step theory provides, at least with the present optical potential.

The calculation of the two-step contribution to the 0_2^+ cross section is complicated by the theoretical uncertainty in the $0_2^+ \rightarrow 2_1^+$ form factor. If we use a pure Kamimu-

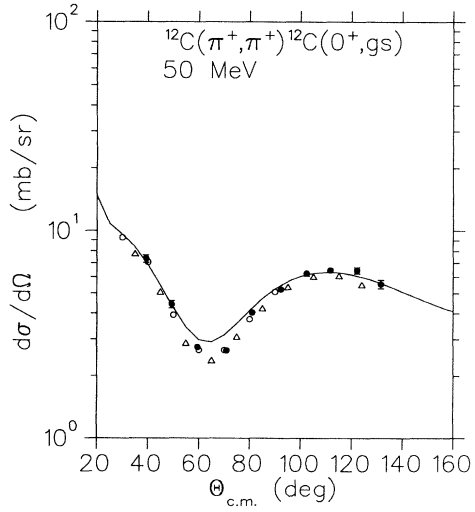

FIG. 6. Elastic (optical model) differential cross sections for ^{12}C(π^+,π^+) at 50 MeV. The data are from Refs. 6, 31, and 8.

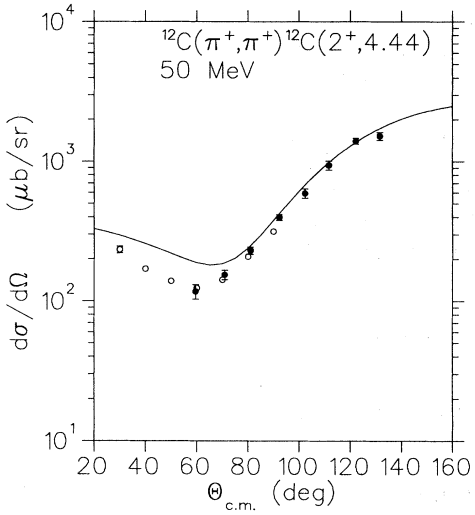

FIG. 7. Inelastic (one-step only) differential cross sections for $^{12}C(\pi^+,\pi^{+'})^{12}C(2^+,4.44$ MeV) at 50 MeV. The data are from Refs. 6, 31 and 8.

ra form factor, but with the strength increased to match the experimental $B(E2)$, i.e., $\beta_2'=1.52$, $\beta_2''=0$ in Eq. (14), we get the wrong sign for the interference, as shown in Fig. 8. This form factor can therefore be considered as ruled out by the data. The interference has the right sign, and agreement with the data is improved over the purely one-step calculation if we use $\beta_2'=1$, $\beta_2''=0.13$. The form-factor mix favored by the data has $\beta_2'=0.8$, $\beta_2''=0.18$; these cross sections are shown in Figs. 9 and 10. This preferred $0_2^+\rightarrow 2_1^+$ form factor is shown in Fig. 5.

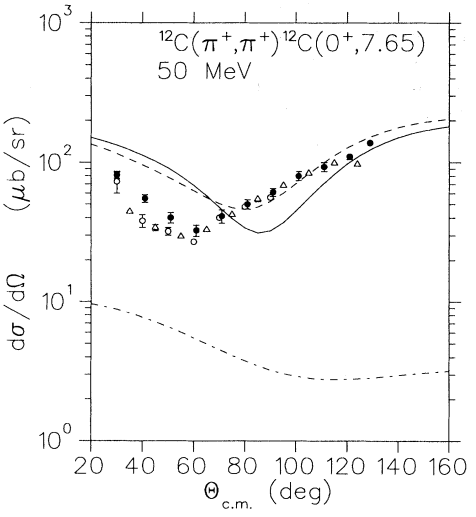

FIG. 8. Inelastic differential cross sections for $^{12}C(\pi^+,\pi^{+'})^{12}C(0^+,7.65$ MeV) at 50 MeV. The dashed line is a purely one-step calculation, the dot-dashed line is a purely two-step ($0_1^+\rightarrow 2_1^+\rightarrow 0_2^+$) calculation using a $\beta_2'=1.52$, and $\beta_2''=0$, and the solid line is the coherent sum of the two mechanisms. The data are from Refs. 6 and 8.

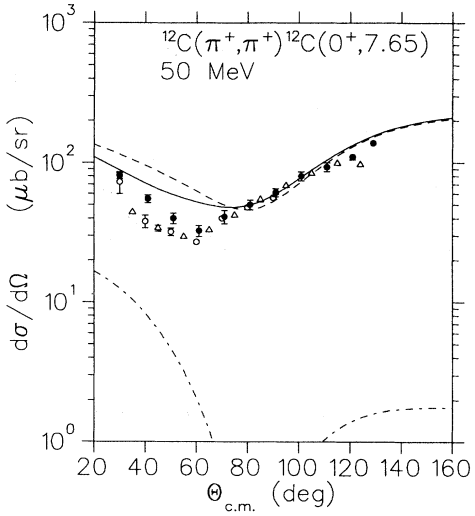

FIG. 9. Inelastic differential cross sections for $^{12}C(\pi^+,\pi^{+'})^{12}C(0^+,7.65$ MeV) at 50 MeV. The dashed line is a purely one-step calculation, the dot-dashed line is a purely two-step ($0_1^+\rightarrow 2_1^+\rightarrow 0_2^+$) calculation using a $\beta_2'=0.8$, and $\beta_2''=0.18$, and the solid line is the coherent sum of the two mechanisms. The data are from Refs. 6 and 8.

VII. CONCLUSIONS

We have taken advantage of the availability of a new pion-nucleus optical potential with a strong EELL parameter[10] to study low-energy inelastic scattering on ^{12}C and ^{28}Si. Since the distortion and absorption are moderate, the pions can penetrate into the nuclear interior. The different cross sections to the low-lying collective states are well predicted without any free parameters, us-

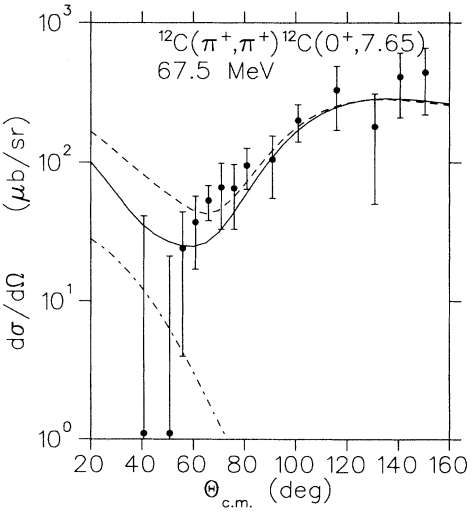

FIG. 10. The same as Fig. 10 but at 67.5 MeV. The data are from Ref. 5.

ing form factors taken from electron scattering. At these energies, the cross sections are particularly sensitive to the form factors near $q \sim 1$ fm^{-1}, that is near their peak; it is not enough to use a reasonable size parameter and a strength fitted to the measured $B(El)$.

The cross sections to the 0_2^+ states are dominated by the one-step mechanism which can explain both the observed magnitude and also, though less well, the shape of the angular distributions. The two-step $0_1^+ \rightarrow 2_1^+ \rightarrow 0_2^+$ amplitude is smaller at all angles and is forward peaked. The interference between these two amplitudes is important, and results are an improved agreement with the data. Again, there is no need to adjust any parameters insofar as they can be extracted from electromagnetic data or well-established theory (e.g., the relative phases). It is interesting to note that this interference can be used to extract information about the form factors connecting excited states, specifically the $2_1^+ \rightarrow 0_2^+$ form factor in ^{12}C.

[1] T. Ericsson and W. Wiese, *Pions and Nuclei* (Oxford University, New York, 1988).

[2] B. K. Jennings and N. de Takacsy, Phys. Lett. **124B**, 302 (1983).

[3] D. A. Sparrow and W. J. Gerace, Phys. Rev. Lett. **41**, 1101 (1978).

[4] C. S. Whisnant, Phys. Rev. C **40**, 1741 (1989).

[5] J. F. Amann, P. D. Barnes, K. G. R. Doss, S. A. Dytman, R. A. Eisenstein, J. D. Sherman, and W. R. Wharton, Phys. Rev. C **23**, 1635 (1981).

[6] L. Lee *et al.*, Phys. Lett. B **174**, 147 (1986).

[7] C. S. Whisnant *et al.*, Phys. Rev. C **39**, 1935 (1989).

[8] B. M. Barnett, H. Clement, W. Gyles, J. Jaki, Ch. Joram, W. Kluge, S. Krell, H. Matthäy, M. Metzler, R. Tacik, G. J. Wagner, and U. Wiedner, Swiss Institute for Nuclear Research Annual Report **20**, 1988; B. Barnett, private communication.

[9] B. G. Ritchie, J. A. Escalante, B. M. Preedom, G. S. Adams, G. S. Blanpied, C. S. Mishra, C. S. Whisnant, J. H. Mitchell, R. J. Peterson, R. L. Boudrie, and D. H. Wright, Phys. Rev. C **41**, 1668 (1990).

[10] O. Meirav, E. Friedman, R. R. Johnson, R. Olszewski, and P. Weber, Phys. Rev. C **40**, 843 (1989).

[11] R. A. Eisenstein and G. A. Miller, Comput. Phys. Commun. **11**, 95 (1976).

[12] H. De Vries, C. W. De Jager, and C. De Vries, At. Data Nucl. Data Tables **36**, 495 (1987).

[13] K. E. Whitner, C. F. Williamson, B. E. Norum, and S. Kowalski, Phys. Rev. C **22**, 374 (1980).

[14] S. W. Brain, A. Johnston, W. A. Gillespie, E. W. Lees, and R. P. Singhal, J. Phys. G **3**, 821 (1977).

[15] A. Nakada and Y. Torizuka, J. Phys. Soc. Jpn. **32**, 1 (1972).

[16] S. Raman *et al.*, At. Data Nucl. Data Tables **36**, 1 (1987).

[17] G. R. Satchler, *Direct Nuclear Reactions* (Oxford University, New York, 1983).

[18] B. H. Wildenthal, Prog. Part. Nucl. Phys. **11**, 5 (1984).

[19] M. Carchidi and B. H. Wildenthal, Phys. Rev. C **37**, 1681 (1988).

[20] S. Das Gupta and M. Harvey, Nucl. Phys. A **94**, 602 (1967).

[21] C. M. Lederer and V. S. Shirley, *Table of Isotopes* (Wiley, New York, 1978).

[22] P. M. Endt and C. van der Leun, Nucl. Phys. A **310**, 208 (1978).

[23] A. Nakada, Y. Torizuka, and Y. Horikawa, Phys. Rev. Lett. **27**, 745 (1971). J. B. Flanz *et al.*, *ibid.* **41**, 1642 (1978); P. Strehl, Z. Phys. **234**, 416 (1970); P. Strehl and Th. H. Shucan, Phys. Lett. **27B**, 641 (1968); H. Crannell, private communication.

[24] S. Cohen and D. Kurath, Nucl. Phys. **73**, 1 (1965).

[25] A. G. M. van Hees and P. W. M. Glaudemans, Z. Phys. A **315**, 323 (1984).

[26] M. Kamimura, Nucl. Phys. A **351**, 456 (1981).

[27] R. Behrman, S. Das Gupta, and N. de Takacsy, Nucl. Phys. A **289**, 397 (1977), and references therein.

[28] F. Ajzenberg-Selove, Nucl. Phys. A **433**, 1 (1985).

[29] U. Wienands *et al.*, Phys. Rev. C **35**, 708 (1987).

[30] G. G. Simon, Ch. Schmitt, F. Borkowski, and V. H. Walther, Nucl. Phys. A **333**, 381 (1980).

[31] R. Sobie *et al.* Phys. Rev. C **30**, 1612 (1984).